Journal of Corrosion and Materials
www.corromat.com

J. Corros. Mater. (2022) 1(2), 123–139.

Spatially Structured Environmental Noise Controls Stability Thresholds in Fractional Corrosion Fields

David J. Sellmyer[1,*], Olivia Bennett[2]

[1] *Nebraska Center for Materials and Nanoscience, University of Nebraska–Lincoln, USA*
[2] *Department of Mechanical Engineering, A. James Clark School of Engineering, University of Maryland, USA*

[*]Corresponding author: dsellmyer@unl.edu
[2] bennettoliv0@gmail.com

(Received: 2 August 2022. Received in revised form: 19 November 2022. Accepted: 5 December 2022. Published online: 30 December 2022.)

Abstract

Since the perturbations of chloride concentration, wetting, dryness, oxygen supply, temperature, and contamination of the surface are unlikely to occur as uniform exposures in space, their organization through coating defects, pores, grains, inclusions, crevices, and exposure zones leads to the possibility that two environments of the same total variance may induce dissimilar corrosion impacts. The framework provides a fractional stochastic reaction-diffusion problem that translates the spatial structure of random exposure into the condition of the mean corrosion activity. In it, the material is modeled by a normalized interval with zero-flux boundary conditions, nonlocal transport is described by the spectral fractional Laplacian, while the environmental forcing acts on the Neumann stable modes. The separation of scales in the system leads to the reduced equation for corrosion activity in which the index of modal susceptibility $\mathcal{S}_r = \sum_{j\in\mathcal{J}} \alpha_j^2/(2Dj^r)$ is the key to obtaining a deterministic term induced by the excitation of random stable modes. The set of numerical experiments includes 600 cases with $D \in \{0.5, 1.0, 1.5, 2.0\}$, $r \in \{1.2, 1.4, 1.6, 1.8, 2.0\}$, $q \in \{1, 2, 3, 4, 5\}$, and $\alpha \in \{0.5, 0.75, 1.0, 1.25, 1.5, 2.0\}$. Two classes of kinetics are considered. With cubic passivation–activation kinetics, the stability of passive state holds whenever $\mathcal{S}_r > 1/3$, whereas in the case of logistic saturated damage, only those equilibria exist for which $\mathcal{S}_r \leq 1/4$ in terms of the normalized carrying capacity. From the performed calculations, one finds that the contribution of low modes dominates threshold crossing: the first mode takes 75 out of 128 cases of cubic stabilization, while the fifth mode only contributes to two cases. The analysis confirms the importance of the spatial distribution of the environmental variability in the fractional corrosion problem.

Keywords: corrosion activity; fractional Laplacian; stochastic reaction–diffusion; modal forcing; passivation threshold; environmental variability.

Keywords: Mappings, convergence, hyperbolic spaces, iteration process.

1. Introduction

While corrosion is generally introduced as an electrochemical phenomenon, the engineering consequences of corrosion emerge in the context of a coupled space-time process, in which reaction rate kinetics, ionic transport, heterogeneity, and fluctuation in exposure conditions interact. The localized nature of corrosion attack, crevice propagation, underfilm damage, reinforcement-depassivation in concrete, and corrosion fatigue is seldom captured by a smooth profile represented in terms of a uniform corrosion rate parameter. A passivating film can be globally intact while a small fraction of defects admit aggressive species. A coated surface may have the same amount of salt deposition as any other surface, just distributed in space differently. A buried pipe may be subject to periodic exposure conditions which vary broadly in time and space. In contrast, a machined surface of an alloy may receive highly frequent microstructural forcing via inclusions and grain boundary chemistries. The question is thus not only the magnitude of the fluctuation but how that fluctuation varies in space.

This is the physical motivation provided by classical corrosion science. Mixed-potential theory provides the physics of anodic and cathodic reactions which give the observed corrosion state [1]. Electrochemical-system analysis relates this to migration, diffusion, and transport [2]. Surface-chemistry analysis further demonstrates the role of passivity and interfacial reactions, which support chemical gradients despite the control of the bulk solution [3]. Localized-corrosion analysis highlights the fact that breakdown of the passive film by itself does not govern persistent pit growth [4]. Further analysis distinguishes the phenomena of initiation, metastability and growth stability through local transport and repassivation criteria [5]. General corrosion analysis emphasizes the interaction of dissolution, chloride accumulation, hydrolysis, geometry and surface film condition [6]. In applications to concrete and infrastructure, critical-chloride analysis demonstrates that depassivation thresholds are distributed instead of pointwise constants [7]. Practical reinforced concrete corrosion guidelines connect this variation to moisture and exposure history [8]. Comprehensive concrete corrosion literature further

relates chloride transport, oxygen access and cracking [9]. These observations motivate the use of mathematical models that maintain the structure of the spatial distribution of environmental influence rather than averaging it into a single environmental forcing term.

Reaction-diffusion models constitute one natural way of describing these processes since they couple reaction rates and local transport. While the corrosion activity variable considered in this study is not intended to represent an electrochemical potential, current density, or pit depth measurements directly, it will be a dimensionless activity field which can represent normalized anodic activity, damage intensity, active site density or aggressive species concentration at a reduced mesoscopic level. Reaction-diffusion theory demonstrates how these reduced variables retain the competition of growth and limitation without the details of the microscopic system [10]. Nonlinear parabolic equation analysis further provides a mathematical basis for these mesoscopic field descriptions [11]. This approach is moreover consistent with the reduced description of passivation, reactant depletion and product layer limitation, where the quantity of interest is the evolution of the damage relevant activity state rather than the full electrochemical description.

Nonlocal transport enters the problem through the fractional Laplacian operator. The general theory of fractional calculus provides the nonlocal operators needed for the description [12]. Fractional differential equations provide an extension of this framework to problems involving memory and anomalous transport [13]. Anomalous diffusion studies demonstrate how the fractional operators capture long-range interactions and non-Fickian spreading [14]. Models of material response further demonstrate their applicability to heterogeneous media [15]. For bounded domains, the spectral definition of the fractional Laplacian is particularly clear, since each Neumann eigenmode is damped proportionally to its wavenumber raised to some power. The operator thus provides a natural connection between the spatial scale of the exposure and the extent to which it influences the mean corrosion state. Different definitions of the fractional operator emphasize that various boundary conditions and interaction properties are encoded into these definitions [16]. Comparative reviews of the spectral versus other fractional Laplacians highlight these differences in bounded domains [17]. This definition is chosen since no-flux boundary conditions and modal attenuation form an essential part of the exposure interpretation.

The stochastic component plays an equally essential role in the model. Environmental variability in the corrosion process is not just noise in the measurements. Wetting and drying, dissolved oxygen, chloride deposition, temperature, biofilm activity, pore connectivity and coating defects are factors that introduce variability which lasts sufficiently long to impact the degradation trajectory. Random dynamical systems theory provides a mathematical framework to describe such random influences [18]. Stochastic process analysis provides the mathematical tools to describe diffusion and Ornstein-Uhlenbeck processes needed for the reduced description [19]. The framework of infinite-dimensional stochastic analysis provides a rigorous setting for the stochastic partial differential equations [20]. The modern stochastic partial differential equations theory provides the relevant existence and regularity framework [21]. When the stable modes decay sufficiently fast compared to a critical slow mode, classical averaging theory allows to reduce their fluctuations to deterministic corrections to the slow dynamics [22]. Multiscale stochastic methods allow for a formalization of this slow-fast reduction [23]. Stochastic bifurcation theory demonstrates how rapidly decaying variables affect the effective dynamics of the slowly decaying variables [24]. The averaging principles provide the theoretical justification for the approximation [25]. This is the analytical heart of the model.

The recent corrosion modeling literature has also been moving towards data rich approaches. Nash et al. provided a review of deep learning in materials degradation and highlighted the need to preserve the mechanistic information in descriptors [26]. Coelho et al. provided a review of machine learning approaches to electrochemical corrosion and emphasized the heterogeneity and scarcity of corrosion observations [27]. Jiang et al. treated the corrosion initiation and propagation as a time series problem and used long short-term memory modeling on 150 days of immersion experiments to predict the corrosion potential evolution [28]. Chen et al. linked the atmospheric corrosion with the time, environment, and material descriptors [29]. These papers demonstrate the increasing reliance on structured descriptors in corrosion prediction, yet the structured environmental forcing remains difficult to describe mathematically. The modal criterion below bridges this gap for a fractional stochastic corrosion field.

The research question thus becomes more specific: given random environmental exposure acting on stable spatial modes of a fractional corrosion-activity field, what modal distributions are capable of changing the mean corrosion state and how do diffusion strength, fractional exponent and forcing amplitude define the transition between the passive stabilization and persistent activity? The answer is derived from a modal susceptibility index, a 600-case calculation grid and two kinetic closures. The model does not aim to simulate the detailed electrochemical behavior. It defines the threshold criterion that the reduced description of corrosion needs to satisfy in order to respect the impact of spatially organized environment.

2. Literature Background

Corrosion models have historically developed along several partially connected paths. The first path is mechanistic electrochemistry, where mass conservation, charge transfer, migration, and diffusion are written directly in terms of potentials, concentrations, and current densities. General corrosion engineering ties these variables to measurable degradation mechanisms [30]. Corrosion-control literature connects them with practical material selection and protection [31]. Electrochemical methods provide the foundation for interpreting interfacial reaction rates [1]. Electrochemical-system theory extends the treatment to ionic transport and coupled field equations [2]. This tradition is indispensable because it ties prediction to measurable thermodynamic and kinetic quantities. Its limitation in structural assessment is that the resulting models can become too detailed for routine uncertainty analysis, especially when local chemistry and microstructure are only partially observed. The second path is empirical or semi-empirical lifetime modeling, in which corrosion rate, pit depth, or cracking risk is related to exposure time, temperature, chloride, humidity, and material class. Such models are useful for engineering prognosis, but they often compress spatial heterogeneity into averaged descriptors. The third path is stochastic and spatial modeling, where corrosion is treated as a random field or a pattern-forming process whose local features interact through transport and reaction. The analysis belongs to this third path while retaining enough analytical structure to produce explicit thresholds.

Localized corrosion makes the need for spatial models especially clear. Pitting and crevice corrosion are initiated at discrete sites, but they can govern the failure of an otherwise intact surface. A critical review of pitting corrosion shows that initiation and metastability depend on local chemistry and passive-film behaviour [4]. Later analysis emphasizes that growth stability and repassivation are controlled by transport constraints as well as the bulk environment [5]. The same logic applies to coated systems and reinforced concrete. A coating holiday or chloride-rich region may occupy only part of the surface but can organize the subsequent degradation path. Critical-chloride reviews show that reinforced-concrete depassivation is spatially variable [7]. Practical assessment guidance links this variability with oxygen access, moisture, and cover condition [8]. Concrete-corrosion literature further connects these factors with cracking and long-term damage [9]. These examples justify the use of a field variable and a no-flux representative interval: the aim is to capture how spatially uneven exposure alters the mean corrosion tendency.

A second body of literature concerns anomalous transport and fractional operators. Fractional-calculus theory gives compact representations of nonlocality and distributed response [12]. Fractional differential-equation models extend these ideas to transport and memory problems [13]. Anomalous-diffusion theory explains how heavy-tailed transport can depart from classical Fickian behaviour [14]. Fractional materials models provide further examples from viscoelasticity and heterogeneous media [15]. For corrosion activity on the normalized interval, the key point is not fractional differentiation in time but fractional damping in space. The spectral fractional Laplacian preserves the modal structure of the Neumann basis while replacing the classical j^2 damping with j^r. This apparently simple change has large interpretive consequences. When r is near two, high spatial modes are strongly suppressed. When r is closer to one, higher modes retain more variance and can contribute more strongly to the mean-field correction. Fractional-Sobolev analysis shows that operator choice is mathematically nontrivial [16]. Reviews comparing fractional-Laplacian definitions further show that the choice should be tied to boundary and transport assumptions [17].

Stochastic averaging provides the third foundation. Random environmental forcing is often treated as an additive disturbance, but nonlinear systems can transform disturbances into systematic drift. Classical averaging theory shows how rapidly relaxing variables can be removed from a slow–fast system [22]. Multiscale stochastic methods provide a systematic formulation of the resulting effective dynamics [23]. Stochastic bifurcation analysis further explains how fast fluctuations modify slow drift [24]. Infinite-dimensional stochastic analysis extends this mechanism to evolution equations [20]. Modern SPDE theory supplies the associated solution framework [21]. Random dynamical-systems theory provides an additional interpretation of the retained averaged influence [18]. The modal susceptibility index used here is a corrosion-specific realization of this logic. It does not merely report the variance of the environment. It reports variance after filtering by the relaxation rate of each stable spatial mode.

Recent data-driven corrosion studies make this analytical perspective timely. Machine-learning reviews show that corrosion observations are often noisy, incomplete, and heterogeneous [26]. More recent corrosion-informatics work demonstrates that physically meaningful descriptors can improve data-driven prediction [27]. Time-series corrosion studies have begun to connect initiation and propagation with temporal descriptors obtained from immersion observations [28]. Atmospheric corrosion models increasingly combine material, time, and environmental variables [29]. These works support the emphasis on structured descriptors. The modal index developed below is not a substitute for data-rich prediction; it is a physically interpretable descriptor that can be estimated from spatial maps and inserted into reduced corrosion kinetics.

3. Corrosion-Activity Setting and Modal Data

The model space is the domain $[0, \pi]$. This normalization is useful since the no-flux eigenfunctions are cosine modes. A physical surface segment $[0, L]$ is converted into $[0, \pi]$ via the transform $x = \pi X/L$. The endpoint no-flux condition implies that the modeled activity takes place in an isolated patch of material in which the activity is exchanged internally on the time scale considered. This assumption is justified for an isolated coating patch, a typical alloy surface segment, or an isolated concrete segment whose variations come mainly from internal transport and reactions.

The state variable $u(t, x)$ is the corrosion-activity field in units of normalized measure. High values stand for strong corrosion and the spatial mean is the damage tendency. The variable is dimensionless so that the structure of the threshold is separated from the material-related scaling. In practical application u may be measured using the scaled local anodic current density, normalized pit density, the signal intensity of corrosion products, or the activity of aggressive species. The exact form of the sensor or imaging modality is not prescribed by the mathematical theory but the scaling must be such that the larger u the higher corrosion-relevant activity.

The environmental influence is described by the stable spatial modes rather than by a uniform noise. This is because exposure is structured in space. Humid band, coating holiday or a region with elevated chlorides is represented by the low wavenumber. Roughness, alternating inclusions or surface defects represent high wavenumbers. The difference is that fractional diffusion attenuates a mode j with the rate j^r. For the constant forcing amplitude, the low modes are less sensitive to damping. Therefore the effect of a fluctuation on the corrosion process is wavenumber-dependent.

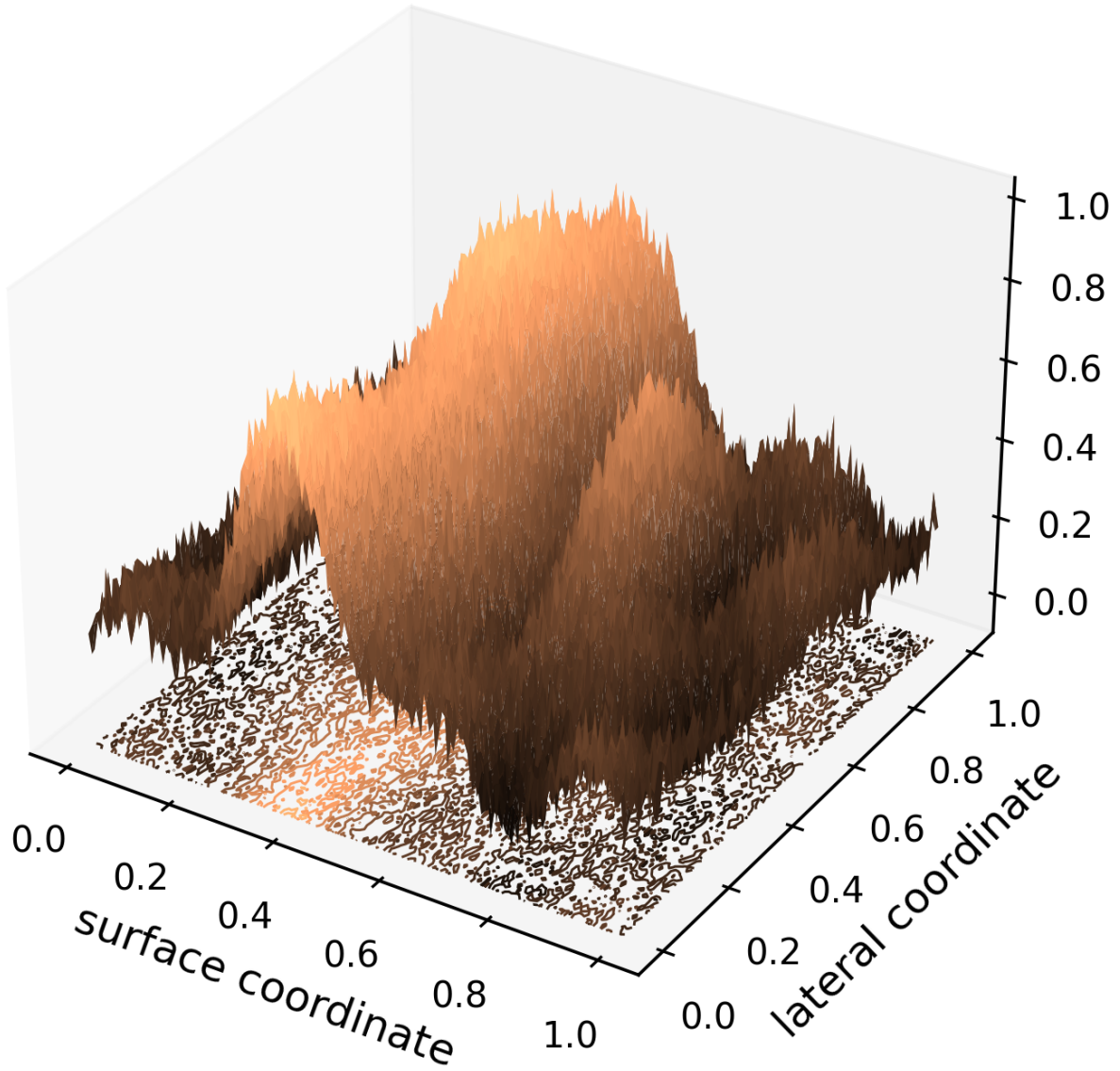

Figure 1: Corrosion-activity topography.

The depicted activity landscape in Figure 1 is the physical realization of the reduced field. The field is represented by a continuous corrosion-activity topography rather than the constant rate constant. The wide bands, mixed defect zones and fine spatial fluctuations are clearly identifiable by their location in the spectrum. The main issue is not the pattern of colors

but the scale of the variation: the same fluctuation level produces the different mean-field outcome due to the fractional damping of the spatial modes.

To make the threshold analysis reproducible, the 600 cases of modal exposure are computed from the parameter grid

$$\mathcal{D}_{\text{grid}} = \{D, r, q, \alpha\} : D \in \{0.5, 1.0, 1.5, 2.0\},\ r \in \{1.2, 1.4, 1.6, 1.8, 2.0\},\ q \in \{1, 2, 3, 4, 5\},\ \alpha \in \{0.5, 0.75, 1.0, 1.25, 1.5, 2.0\}. \tag{1}$$

There are 600 cells within the grid. The information recorded in each cell is the susceptibility parameter $\mathcal{S}_r$, the cubic passivation parameter, the logistic positive-equilibrium parameter, the cubic critical amplitude parameter, and the two logistic equilibrium parameters where there are any. The grid is calculated data that illustrates the interaction between the position of the modes, diffusion, fractional exponent, and forcing amplitude.

Table 1: Computation grid.

Component	Values or definition	Modeling role
Diffusion strength	$D = 0.5, 1.0, 1.5, 2.0$	Stable-mode relaxation
Fractional exponent	$r = 1.2, 1.4, 1.6, 1.8, 2.0$	Modal damping slope
Forced mode	$q = 1, 2, 3, 4, 5$	Exposure wavelength
Forcing amplitude	$\alpha = 0.5, 0.75, 1.0, 1.25, 1.5, 2.0$	Environmental variance
Recorded outputs	$\mathcal{S}_r$, threshold indicators, critical amplitudes, logistic roots	Reduced response variables

The entries of Tab. 1 are what defines the whole computational evidence that has been used in the result. The purpose of using the grid here is to separate amplitude from the position of the mode. In this case, it makes it possible to eliminate any form of uncertainty that usually comes with interpreting results in terms of exposure to corrosion since a rough surface does not necessarily imply a greater impact on the mean compared to a smoother one because of fractional damping.

4. Fractional Spectral Model

The governing field equation is expressed as

$$\mathrm{d}u = \Big[-D(-\Delta_N)^{r/2}u + P(u)\Big]\ \mathrm{d}t + \sum_{j\in\mathcal{J}} \alpha_j e_j(x)\ \mathrm{d}W_j(t), \qquad 1 < r \le 2, \tag{2}$$

where $D > 0$ is the diffusion coefficient, P is a nonlinear corrosion-activity reaction law, W_j are independent standard Wiener processes, and $\mathcal{J}$ is a finite set of forced stable modes. The Neumann eigenfunctions are

$$e_0(x) = \pi^{-1/2}, \qquad e_j(x) = \sqrt{2/\pi}\cos(jx), \quad j \ge 1. \tag{3}$$

The spectral fractional Laplacian is defined by

$$(-\Delta_N)^{r/2}e_0 = 0, \qquad (-\Delta_N)^{r/2}e_j = j^r e_j, quadj \ge 1. \tag{4}$$

The zero mode is undamped because it represents the spatial mean. Stable modes are damped at rates Dj^r. This is the precise location at which spatial scale enters the reduced corrosion dynamics.

The field is decomposed into a spatial mean and stable fluctuations,

$$u(t, x) = \xi(t)e_0(x) + v(t, x), \qquad \langle v, e_0\rangle = 0. \tag{5}$$

The mean amplitude $\xi(t)$ represents the principal state of large-scale corrosion, while $v(t, x)$ is responsible for structured variations. Upon insertion of such a representation into Eq. (2), one separates the critical undamped mode from the stable modes. This model is referred to as the critical one because the spatial mean is not damped by diffusion and its dynamics depend both on the reaction kinetics and on the averaged effect of the stable stochastic modes.

Modal decomposition of the field map given in Fig. 2 clarifies how the no-flux basis separates broad from fine scale. The spatial mean is the undamped mode, and all the higher-order Neumann modes are responsible for structured variation caused by the nonuniformity of exposure. Such a distinction is necessary because a single number characterization of the corrosion rate will equate two surfaces with the same variance, but different structures – either a broad chloride band or fine roughness.

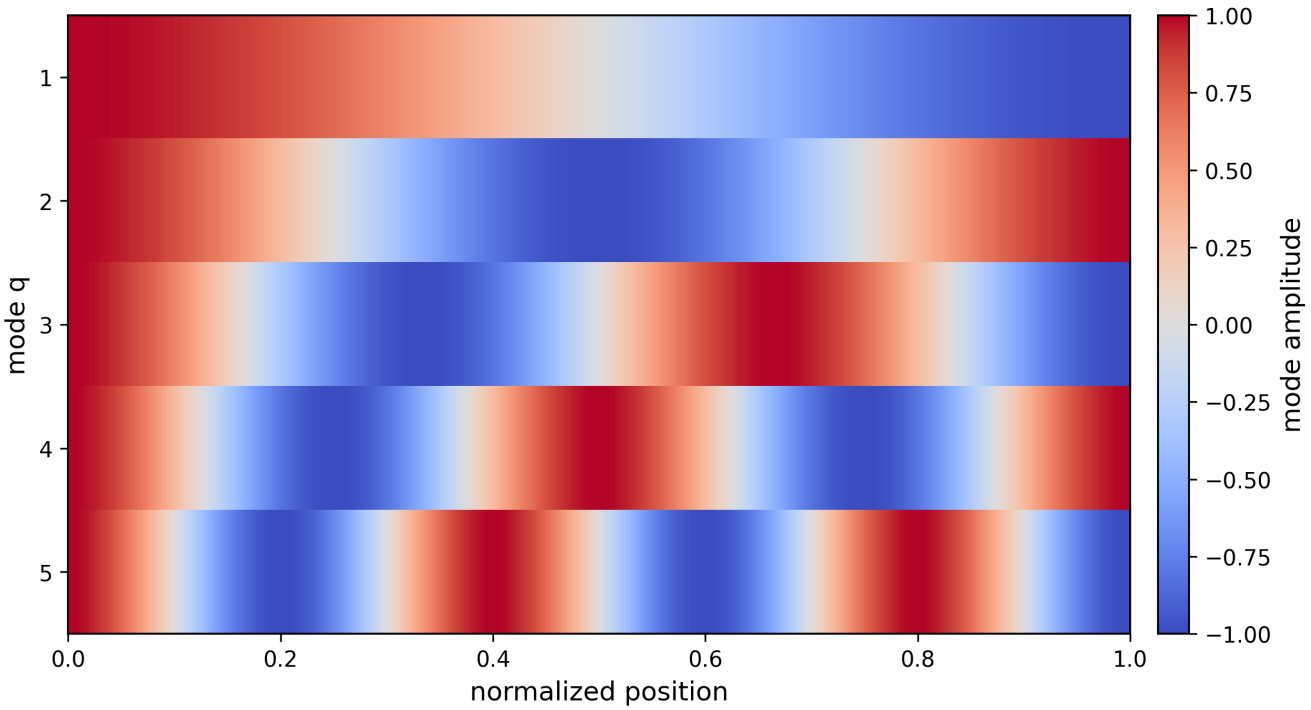

Figure 2: Neumann-mode field map.

In the fast stable-mode regime, each forced stable coefficient $z_j(t)$ is approximated by an Ornstein–Uhlenbeck process,

$$\mathrm{d}z_j = -Dj^r z_j \,\mathrm{d}t + \alpha_j \,\mathrm{d}W_j(t), \qquad j \in \mathcal{J}. \tag{6}$$

The stationary second moment is

$$\mathbb{E}z_j^2 = \frac{\alpha_j^2}{2Dj^r}. \tag{7}$$

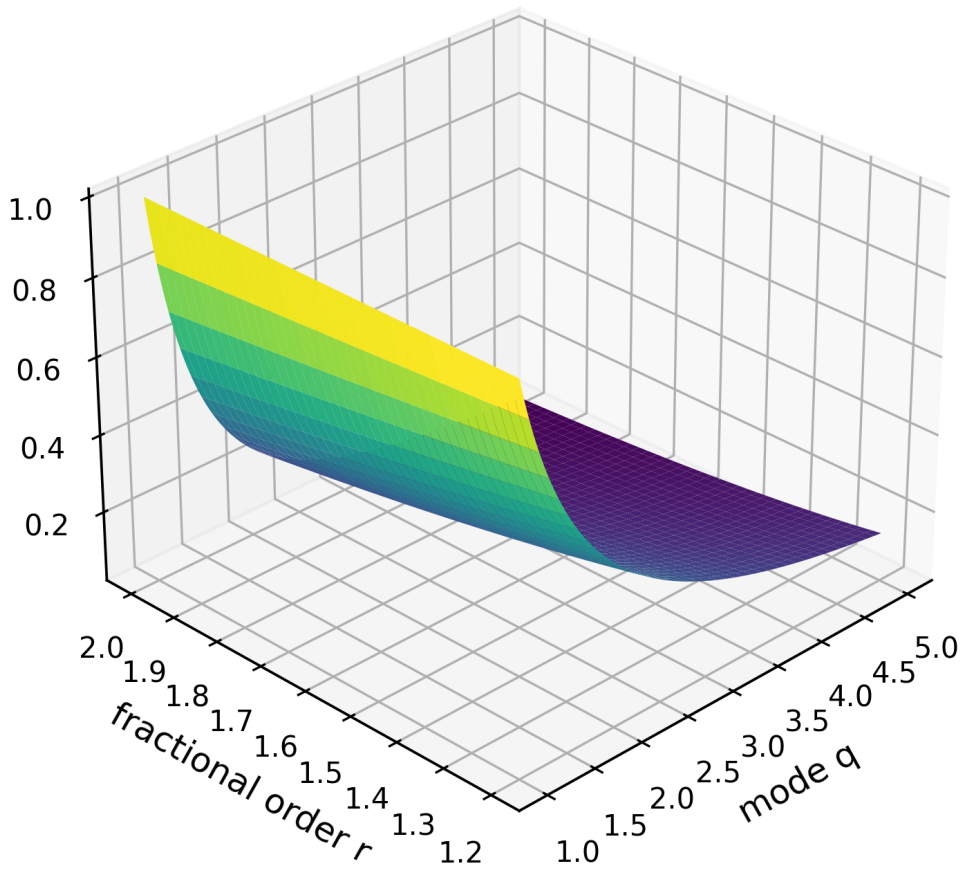

Figure 3: Fractional attenuation surface.

Summing the modal variances gives the susceptibility index

$$\mathcal{S}_r = \sum_{j \in \mathcal{J}} \frac{\alpha_j^2}{2Dj^r}. \tag{8}$$

This can be simplified further for the case of a single forced mode q to become $\mathcal{S}_r = \alpha^2/(2Dq^r)$. The meaning of this index is clear from a physical standpoint; it is the fraction of variance that survives the effect of fractional diffusion and can still be seen by the mean corrosion process.

The figure below shows how the attenuation of the surface explains the importance of the effect of $2Dj^r$. The stationary variance of the mode is high if the forcing is high, the diffusion is low, and the wavenumber of the mode is low. If both q and r are increased, then the contribution of the same environmental fluctuations will decrease to $\mathcal{S}_r$.

5. Mean-Field Reduction and Kinetic Closures

Given a polynomial function P for the reaction rate, the stochastic averaging over the fast stable field results in a deterministic correction in the equation for the critical mode. If we denote the even-order moments of the stable field as $M_{2\ell}$, then

$$\frac{\mathrm{d}\xi}{\mathrm{d}t} = P(\xi) + \sum_{\ell=1}^{\lfloor m/2 \rfloor} \frac{M_{2\ell}}{(2\ell)!} P^{(2\ell)}(\xi), \tag{9}$$

where m is the degree of P. The second moment dominates due to the zero odd moments of centered Gaussian stable processes. In the modal exposure approach, the second moment can be represented by $\mathcal{S}_r$. This simplified equation is not offered as a purely empirical fit to some curve. The theory of semigroups offers the framework for splitting dissipative evolutionary equations into slow and stable parts [32]. Analysis of infinite-dimensional dynamical systems offers another justification for modal simplification [33]. Finally, multiscale stochastic analysis justifies the influence of fast stable modes on the slow process [23].

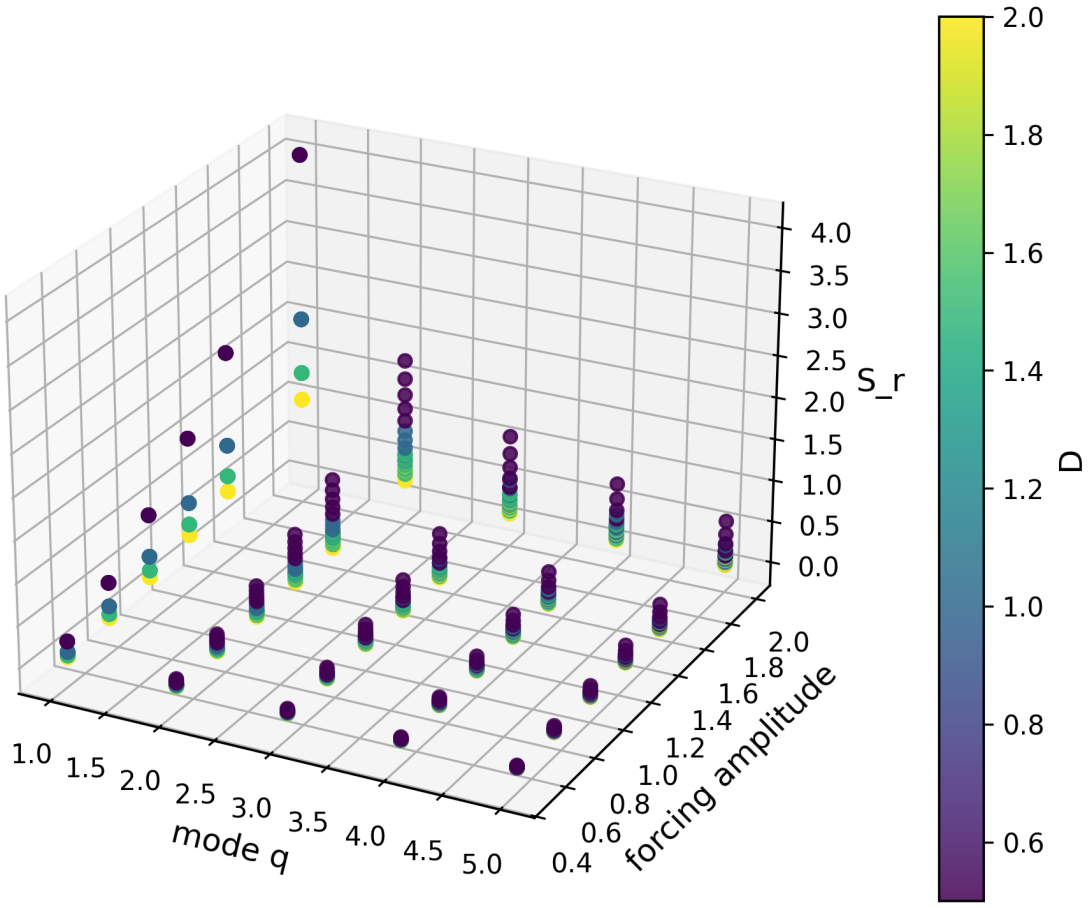

Figure 4: Susceptibility across 600 cases.

The susceptibly cloud in Fig. 4 shows the entire 600 cases computed prior to kinetic threshold application. The large values cluster in the region of low mode, high amplitude, and low diffusion within the parameter space. The distribution

ensures that the reduction does not put all random fields of exposure on an equal footing but only the part of the field which survives damping by fractionation can shift the mean corrosion activity equation.

The first kinetic closure is a cubic passivation-activation law,

$$P(u) = u - u^3. \tag{10}$$

The positive linear term describes the activation effect of a small corrosion activity regime when there are favorable electrochemical conditions. The cubic limitation is associated with passivation, reactant consumption, corrosion product occlusion, or saturation of active sites. Semilinear parabolic equations are justified for cubic normal forms in proximity to an instability threshold [32]. Infinite dimensional dynamical systems theory employs similar equations for symmetry breaking and saturation effects [33]. Insertion into Eq. (9) yields

$$\frac{\mathrm{d}\xi}{\mathrm{d}t} = (1 - 3\mathcal{S}_r)\xi - \xi^3. \tag{11}$$

The passive state is locally stabilized when the effective linear coefficient becomes negative, namely

$$\mathcal{S}_r > \frac{1}{3}. \tag{12}$$

For a single forced mode, the critical amplitude is

$$\alpha_{\mathrm{crit}} = \sqrt{\frac{2Dq^r}{3}}. \tag{13}$$

This formula is central because it expresses the environmental amplitude required for passive stabilization as a function of diffusion, fractional exponent, and spatial mode.

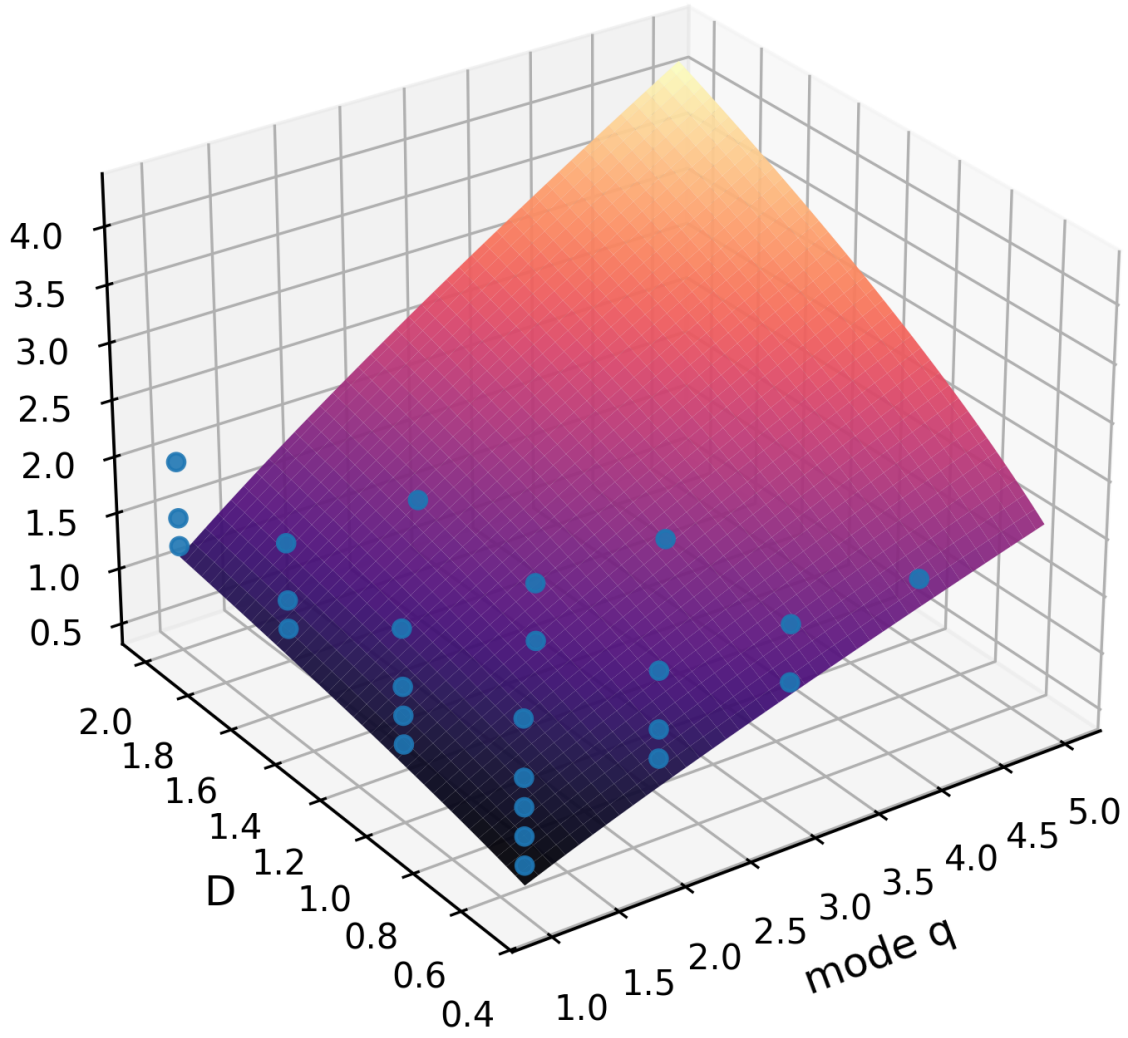

Figure 5: Cubic stabilization surface.

The passivation boundary in Fig. 5 indicates the point at which the stability of the cubic passivation state shifts. Those points that have $\mathcal{S}_r > 1/3$ happen mostly for small mode number and high amplitude of forcing. Increase in diffusion or

increase in fractional exponent leads to the increase in amplitude needed for the modes above the first one. This graph makes Eq. (13) a straightforward tool for testing the ability of exposure wavelength to change the mean state.

The second kinetic model is the logistic damage growth,

$$P(u) = Au\left(1 - \frac{u}{K}\right), \qquad A > 0, \quad K > 0. \tag{14}$$

This model is suitable when the activity increases linearly with low activity but is bounded by the finite amount of reactants, passivation, blocking of the surface by product layers, or geometric saturation. Fisher's model is a typical simplified model for saturated growth and front propagation [34]. The Kolmogorov–Petrovsky–Piskunov model presents the traveling wave approximation [35]. Reaction diffusion theory additionally proves the widespread application of logistic kinetics to growth problems [10]. Averaging gives

$$\frac{\mathrm{d}\xi}{\mathrm{d}t} = A\xi\left(1 - \frac{\xi}{K}\right) - \frac{A}{K}\mathcal{S}_r. \tag{15}$$

Positive equilibria satisfy

$$\xi_{\pm} = \frac{K}{2}\left(1 \pm \sqrt{1 - \frac{4\mathcal{S}_r}{K^2}}\right), \tag{16}$$

so a positive equilibrium pair exists only when

$$\mathcal{S}_r \le \frac{K^2}{4}. \tag{17}$$

For the normalized calculation with $K = 1$, the critical value is $\mathcal{S}_r = 0.25$.

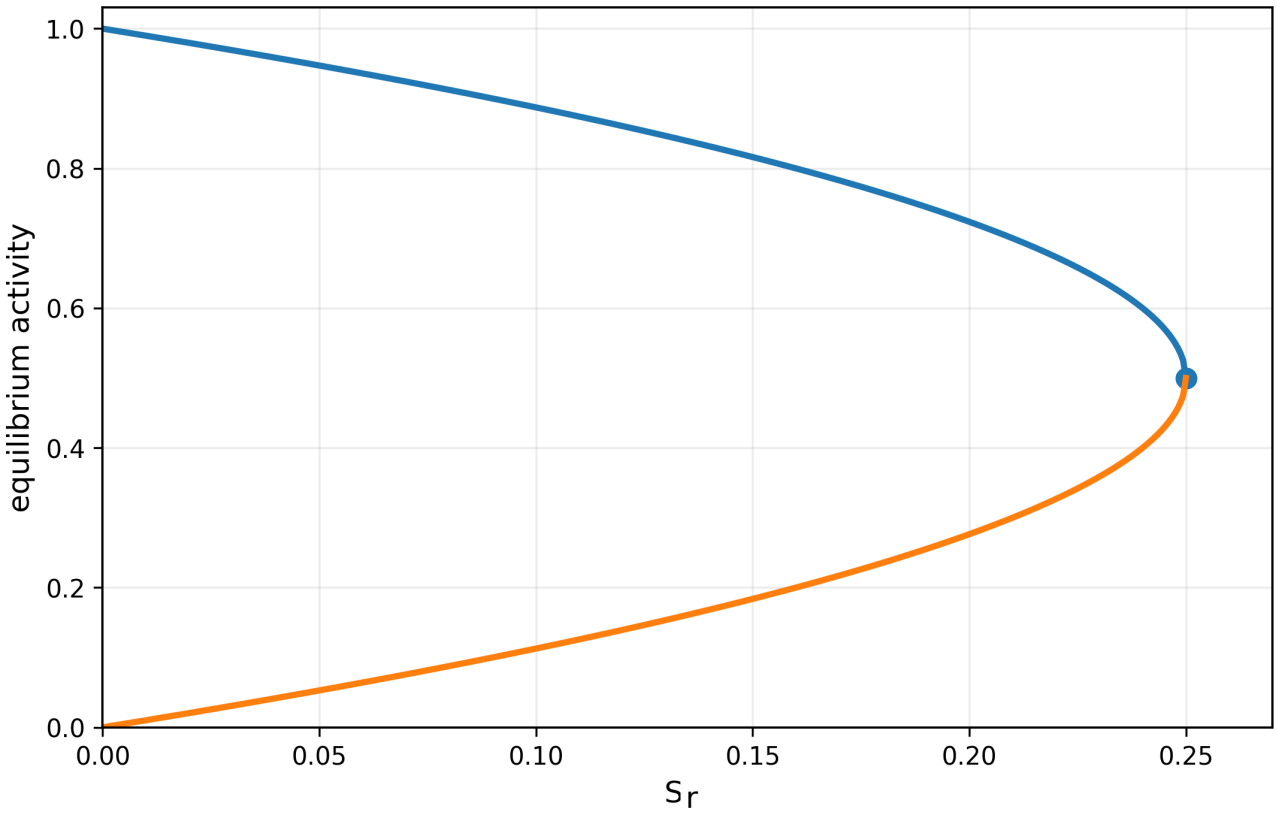

Figure 6: Logistic equilibrium compression.

The equilibrium curves depicted in Figure 6 give the saturated-growth complementary explanation. With increasing $\mathcal{S}_r$, the upper root gets smaller and the lower one gets larger until the two coincide for $\mathcal{S}_r = 0.25$ at $K = 1$. This compressed gap between the roots is the mathematical description of less persistence of the positive active state. Low mode exposure impacts the logistic closure equation by eliminating the pair of equilibria at positive values rather than altering their magnitude.

6. Results and Discussion

The computations utilize the equations mentioned above, along with the dataset of 600 cases described by Eq. (1). Below are the graphs that show the same computed results of the susceptibility, threshold indicators, and equilibrium roots. The reference parameters used in the analytical plots are $D = 1$, $A = 1$, and $K = 1$, except when indicated otherwise. These

results are deterministic outcomes of the modal analysis and thus serve as a well-controlled framework for understanding the effects of spectral exposure on the mean-field dynamics. They should not be considered fitting estimates of a specific alloy. Their importance lies in demonstrating what combinations of the modal scale, diffusion rate, fractional exponent, and amplitude cross corrosion-relevant thresholds.

Table 2: Cubic amplitudes.

Forced mode q	$r = 1.2$	$r = 1.6$	$r = 2.0$
1	0.816	0.816	0.816
2	1.238	1.422	1.633
3	1.578	1.966	2.449

The values in Tab. 2 suggest that the first mode has unique properties due to the fact that $1^r = 1$. Its critical amplitude will always be 0.816 regardless of the value of fractional exponent r, for $D = 1$. This is different for the second and third modes. In particular, for $q = 2$ the threshold grows from 1.238 at $r = 1.2$ to 1.633 at $r = 2.0$. And for $q = 3$ from 1.578 to 2.449. The increasing gap between the thresholds suggests that the exponent changes not only the diffusion constant but also the ability of short-wavelength forcing to affect the mean corrosion state. Classical diffusion causes strong suppression of the high modes. Fractional damping allows higher modes to retain their susceptibility.

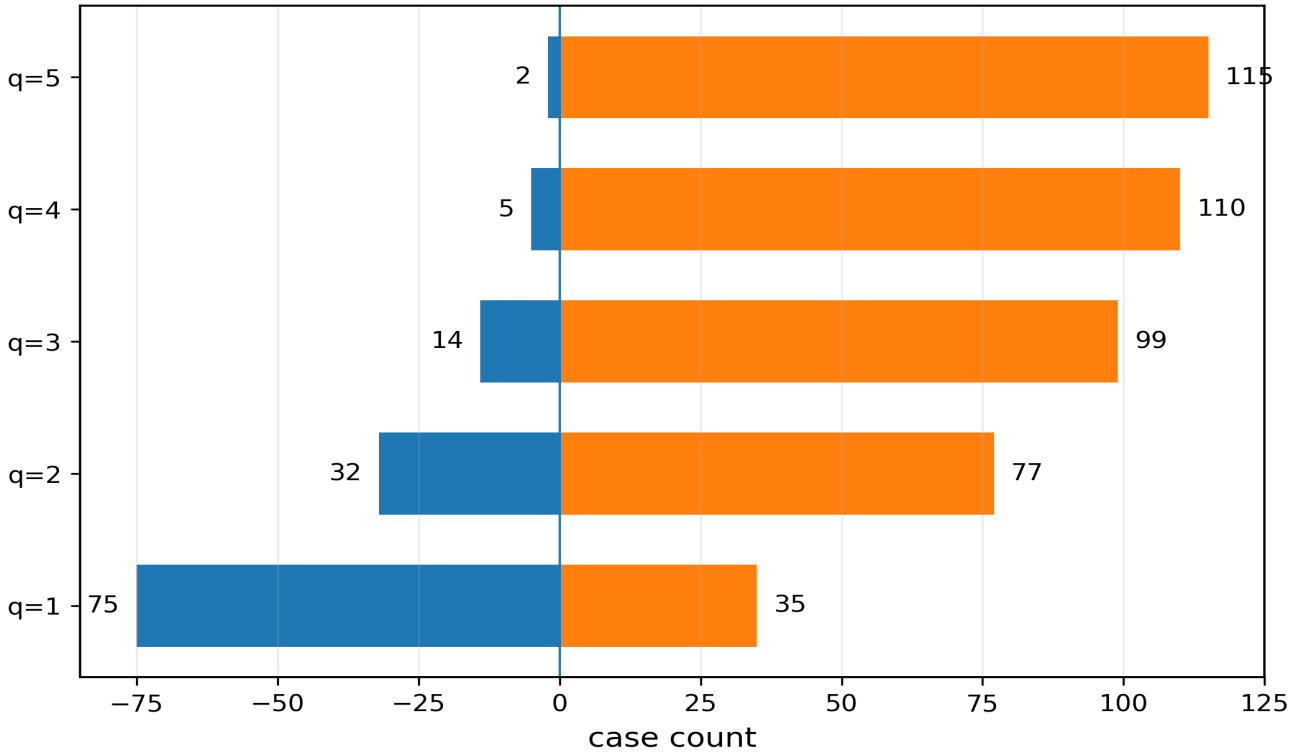

Figure 7: Mode-wise threshold outcomes.

The number of outcomes in Fig. 7 illustrates the response of the kinetic closures to the forcing modes. The cubic law has predominantly the first mode contributing 75 outcomes out of 128 stable cases. Logistic closure shows opposite tendency since the positive roots are most frequently found at the fourth and fifth modes where the susceptibility of modes is low. The paired plot view highlights the fact that both closures detect broad exposure as the main driver of the mean-state evolution although different events are mathematically counted in each case.

Table 3: Spectral weights.

Mode j	$r = 1.2$	$r = 1.6$	$r = 2.0$
1	1.000	1.000	1.000
2	0.435	0.330	0.250
3	0.268	0.172	0.111
4	0.189	0.109	0.063
5	0.145	0.076	0.040

The attenuation coefficients in Tab. 3 allow us to consider the influence of the fractional power independently of the other

parameters. While the fifth mode keeps its weight equal to 0.145 with respect to the first one at $r = 1.2$, it is only 0.040 at $r = 2.0$. Therefore, the reason why the fractional non-local transport leads to the greater relevance of the intermediate and high modes lies within this difference. In particular, this becomes especially important for the application to corrosion processes in materials characterized by complex pore structure, coating inhomogeneity, roughness, or heterogeneity of products layers. The model fixing the value of $r = 2$ could underestimate the mean-field effect of high-mode exposure.

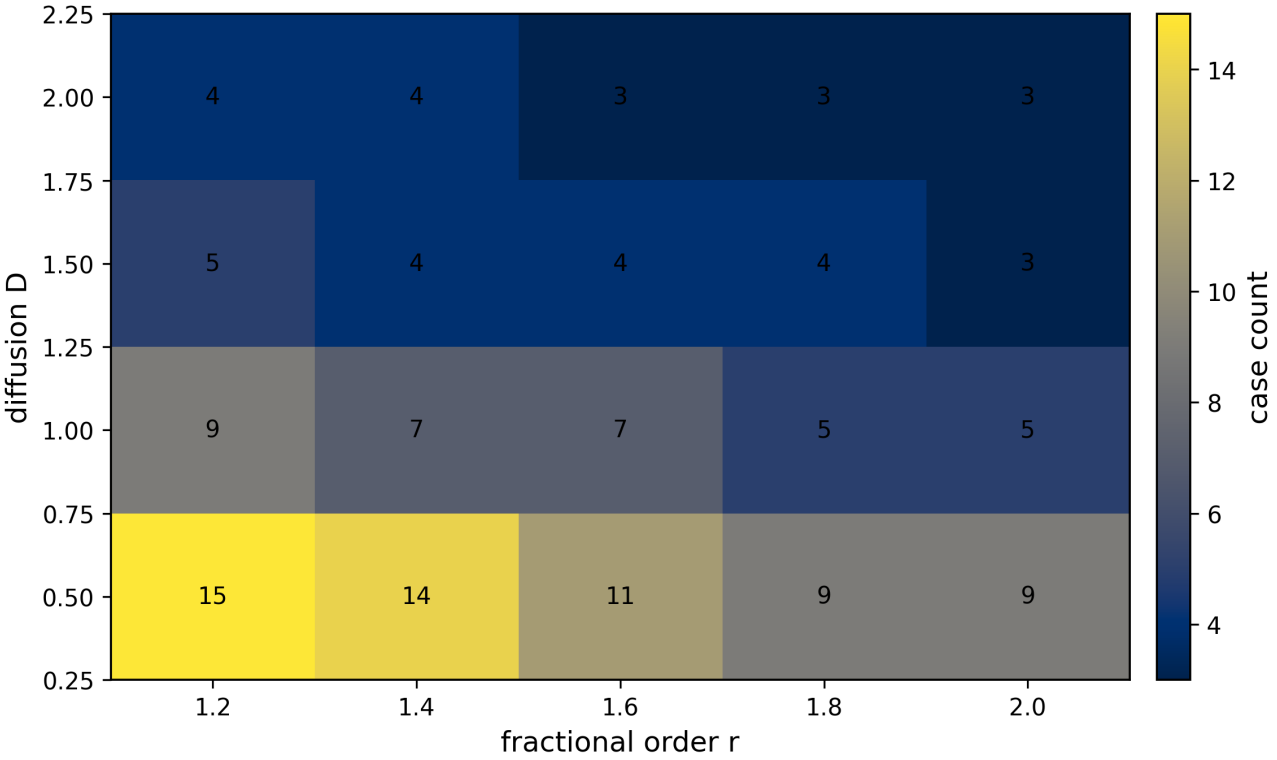

Figure 8: Transport-parameter outcome counts.

The analysis of the mode transportation outcomes in Figure 8 separates the influences of diffusion power and the fractional order of the Laplacian. First, the number of stabilizing cases decreases from 58 for $D = 0.5$ to 17 for $D = 2.0$. Second, it also reduces as r grows from 1.2 to 2.0. The reasons behind these differences are completely different: the diffusion power D scales all stable variances of modes inversely, whereas the parameter r discriminates against higher modes using the coefficient q^{-r}. Hence, we come to the conclusion that the diffusion power and the fractional order cannot be united into a single damping parameter empirically.

The full grid of 600 cases allows us to perform a more reliable check of the three-mode threshold than Table **??**. Out of all possible combinations, there are 128 cases of stabilization according to the cubic criterion $\mathcal{S}_r > 1/3$ and 472 cases of instability. The distribution of the first 128 cases in modes is highly unbalanced: 75 cases correspond to the first mode, 32 to the second one, 14 to the third one, five to the fourth mode, and two to the fifth mode. As a result, 58.6% of all cases correspond to the first mode only, and 5.5% to the fourth and fifth modes altogether. Thus, we see that the advantage of low modes is not just an accidental property of the formula being plotted.

Table 4: Grid outcomes.

Mode q	Cubic stabilized	Cubic share	Logistic roots	Logistic share
1	75/120	62.5%	35/120	29.2%
2	32/120	26.7%	77/120	64.2%
3	14/120	11.7%	99/120	82.5%
4	5/120	4.2%	110/120	91.7%
5	2/120	1.7%	115/120	95.8%

Mode-wise results from Tab. 4 highlight the complementarity of the two kinetic closures. The low modes stabilize the cubic passive regime more often because the resulting values of $\mathcal{S}_r$ are typically larger. On the other hand, the condition $\mathcal{S}_r \leq 0.25$ is much harder to satisfy at higher modes. Thus, the low modes rarely destabilize the cubic law but often destabilize the logistic positive pair. From the corrosion point of view, the large-scale environmental disturbances are able to change the mean metal activity, while small-scale variations tend to remain local unless the fluctuations are strong or

the diffusion coefficient is small. It might be helpful for understanding why some spatially extended exposure patterns can affect the overall corrosion trend, while the fine-spatial roughness influences mostly the local behavior.

Cross-counts also demonstrate that some combinations of parameters are highly sensitive. In particular, at the first mode, each combination of $\alpha = 1.25$, 1.50, and 2.00 is able to stabilize the cubic law for all four diffusivities and all five values of the exponent, yielding 20 stabilizing cases for each of these amplitudes. Stabilization starts only at $\alpha = 1.00$ at the second mode, where two cases are found to exceed the critical value of $\mathcal{S}_r$, and becomes 16 for $\alpha = 2.00$. In turn, the third mode demands an even higher forcing – no cases are found below $\alpha = 1.25$, and only 9 cases are found at $\alpha = 2.00$. Finally, the contribution from the fourth and fifth modes is possible only at high amplitudes. One can see that these results give a natural physical order: the broad exposure zones are able to modify the mean behavior even at relatively low amplitude, while the fine-spatial fluctuations have to be very strong to do that.

As expected, the influence of diffusion depends strongly on its strength. In the entire parameter space, there are 58 cases of cubic stabilization with $D = 0.5$, 33 with $D = 1.0$, 20 with $D = 1.5$, and 17 with $D = 2.0$. Higher diffusion leads to the smaller stationary variance of the stable modes and, hence, makes the transition through the critical threshold less likely. The decrease is the strongest between $D = 0.5$ and $D = 1.0$ because the susceptibility index decreases with the diffusion coefficient. After $D = 1.0$, the remaining cases of stabilization are already confined to low modes and high amplitudes, which results in a slower decline.

Table 5: Diffusion cutoff.

Diffusion coefficient D	Cubic stabilized cases	Stabilized share
0.5	58/150	38.7%
1.0	33/150	22.0%
1.5	20/150	13.3%
2.0	17/150	11.3%

The trend shown in Tab. 5 corresponds directly to a certain design choice. A material or coating that favors lateral spreading of the aggressive species will suppress the capability of a structured environmental fluctuation to shift the mean state. Nevertheless, the model does not suggest that increased diffusion is always favorable in all electrochemical aspects. In a complete model, a higher diffusion coefficient would also provide access to more reactants or remove more inhibitors. The reduced model yields a more specific prediction: stronger damping of the stable modes decreases the stochastic term in the mean-field dynamics according to the given activity equation.

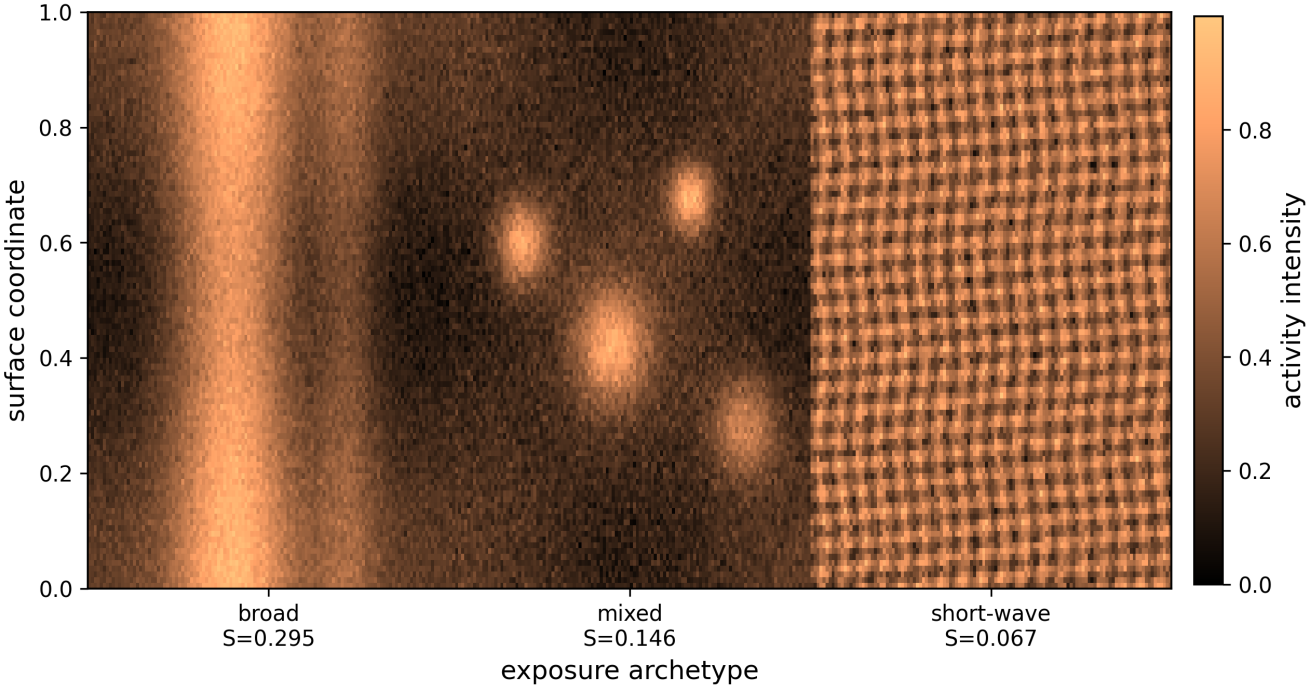

Figure 9: Exposure morphology and weighted impact.

The comparison of exposure morphologies in Figure 9 relates the numeric thresholds to the physically meaningful surface structures. For $D = 1$ and $r = 1.6$, the broad humidity band gives $\mathcal{S}_r = 0.295$, the defect field gives $\mathcal{S}_r = 0.146$, and the roughness field gives $\mathcal{S}_r = 0.067$. Neither the roughness of the structure nor any other property determines the

order. Instead, it is determined by how much of the fluctuation resides in the lower spatial modes that survive fractional relaxation.

The fractional exponent also makes a difference for the grid calculations. There are 33 stabilized cases among 120 at $r = 1.2$, 29 at $r = 1.4$, 25 at $r = 1.6$, 21 at $r = 1.8$, and 20 at $r = 2.0$. The monotonically decreasing series indicates an increased stability provided by the stronger damping of higher modes as the exponent grows. The fairly minor difference between $r = 1.8$ and $r = 2.0$ occurs because the vast majority of the remaining cases reside in the first mode, where $j^r = 1$ regardless of r. The fractional exponent plays a role when there are modes besides the first in the exposure pattern. Such result becomes particularly important for a rough or multiphase surface, where environmental fluctuations need not be dominated by a single broad band.

The amplitude effect is nonlinear because the cubic threshold is determined by α^2. In the grid, there is no stabilized case with $\alpha = 0.5$, while 51 cases out of 100 stabilize the law at $\alpha = 2.0$. The intermediate amplitudes demonstrate the gradual transition: five cases at $\alpha = 0.75$, 12 at $\alpha = 1.0$, 28 at $\alpha = 1.25$, and 32 at $\alpha = 1.5$. The logistic condition acts in the opposite way. All 100 cases with $\alpha = 0.5$ have positive logistic roots, whereas 38 of 100 cases with $\alpha = 2.0$ have them. Asymmetric nature of the behavior indicates that an identical increase in the exposure amplitude can be viewed both as the stabilization of the cubic passivation law and the destruction of the positive logistic equilibrium pair. It all depends on the regime.

The numerical range of the susceptibility index also provides information about the seriousness of modal placement. The lowest value in the computation is $\mathcal{S}_r = 0.0025$, obtained for $D = 2.0$, $r = 2.0$, $q = 5$, and $\alpha = 0.5$. At the corresponding end of the range, the forcing survives the stable-mode damping to such extent that the cubic equation still operates and the logistic roots remain close to their values in the absence of the forcing. The highest value is $\mathcal{S}_r = 4.0$, obtained for any combination of $D = 0.5$, $q = 1$, and $\alpha = 2.0$, irrespective of r because the first mode satisfies the identity $1^r = 1$. The range 0.0025 to 4.0 cannot be obtained solely due to the variation of the total variance; it appears due to the shifting of the same random exposure along the scales of modal wavelengths and diffusion exponents. Thirty-five cases have $\mathcal{S}_r > 1.0$, and all these cases lie far beyond both the cubic threshold and the logistic value of the root collision. On the contrary, 178 cases have $\mathcal{S}_r \leq 0.05$, where the reduced kinetics is only weakly affected by the forcing.

The logistic calculations demonstrate the same parameter dependence from the opposite side of the threshold. The saturated positive pair of roots is preserved in 82 of 150 cases at $D = 0.5$, 104 at $D = 1.0$, 120 at $D = 1.5$, and 130 at $D = 2.0$. Higher diffusion coefficient, thus, preserves the positive pair more often because it reduces the variance of the modes entering the mean-field equation. Even more striking is the variation of the counts of the forced modes. The positive pair of roots is preserved in the first mode in 35 of 120 cases, in the second mode in 77 cases, in the third mode in 99 cases, in the fourth mode in 110 cases, and in the fifth mode in 115 cases. Such a behavior is not contradictory. The cubic equation indicates when the strong modal susceptibility stabilizes the passive state; the logistic equation indicates when the strong modal susceptibility removes the positive equilibrium pair. Both laws single out the same broad-band exposures as the drivers of the mean-state change.

The dependence on the exponent is most pronounced off the first mode. Across the 600 calculations, the saturated logistic positive roots are preserved in 77 cases at $r = 1.2$, in 84 cases at $r = 1.4$, in 88 cases at $r = 1.6$, in 91 cases at $r = 1.8$, and in 96 cases at $r = 2.0$. The increasing number of the cases is directly caused by the increased damping of the higher spatial modes as the exponent grows. The number of the cubic cases decreases correspondingly, from 33 down to 20, because fewer modal combinations can exceed the threshold $\mathcal{S}_r > 1/3$ when high-mode weights become smaller. Such two series of values provide a concrete interpretation of the fractional order in the corrosion problem: a smaller exponent does not just make transport "slower" or "faster" in some vague manner; it changes which wavelengths matter after the stable-mode relaxation.

Table 6: Logistic roots.

$\mathcal{S}_r$	ξ_-	ξ_+	State interpretation
0.00	0.000	1.000	Full positive state
0.05	0.053	0.947	Weak compression
0.10	0.113	0.887	Moderate compression
0.20	0.276	0.724	Strong compression
0.25	0.500	0.500	Root collision

The saturated growth is captured numerically by the root pairs in Tab. 6. Namely, as $\mathcal{S}_r$ goes up from 0 to 0.20, the upper positive equilibrium decreases from 1.000 to 0.724, whereas the lower one rises from 0 to 0.276. For $\mathcal{S}_r = 0.25$, the equilibria become equal and collapse into 0.500. When $\mathcal{S}_r$ exceeds this critical value, the reduced logistic equation does not have positive roots anymore. This is another possible way for structured fluctuations to deprive corrosion processes of their

stable saturated activity. However, this effect must be considered at the reduced activity variable level, not the physical disappearance of the corrosion reaction itself.

For composite forcings, examples show why the mode distribution is crucial. If $D = 1$ and $r = 1.6$, then the low-mode humid zone with $\alpha_1 = 0.70$ and $\alpha_2 = 0.55$ leads to $\mathcal{S}_r = 0.295$, i.e., close to the cubic transition and beyond the logistic root existence condition. The defect field where $\alpha_1 = \alpha_2 = \alpha_4 = 0.45$ yields $\mathcal{S}_r = 0.146$ and destabilizes the cubic passive state while preserving the logistic positive equilibrium pair. The short-wave roughness example with $\alpha_4 = \alpha_5 = 0.85$ has $\mathcal{S}_r = 0.067$, even with larger mode amplitudes in the latter case.

Table 7: Composite cases.

Case	Modal amplitudes	$\mathcal{S}_r$ at $r = 1.6$	Reduced implication
Broad humid band	$\alpha_1 = 0.70,\ \alpha_2 = 0.55$	0.295	Near cubic transition
Mixed defect field	$\alpha_1 = \alpha_2 = \alpha_4 = 0.45$	0.146	Positive pair retained
Short-wave roughness	$\alpha_4 = \alpha_5 = 0.85$	0.067	Weak mean correction

These composite cases are particularly pertinent to inspection measurements. A visual or sensor measurement of surface heterogeneity could emphasize small-scale roughness over large-scale discoloration, while the reduced model indicates that the former might be less significant for the mean activity than the latter. This is not meant to devalue the role of the high modes. The high modes might dictate local hazard onset, micro-cracking, or pit shape. What we want to say is that the influence of the former on the mean-field stochastic correction is moderated by the fractional damping mechanism. A proper corrosion assessment therefore requires a distinction between local hazard descriptors and mean-state susceptibility descriptors.

The remaining part of the averaging reduction depends on the separation between the relaxation of the stable mode and the slow evolution of the mean field. The reduction works best if the quantity Dj^r is large for the forced stable modes or the amplitude is sufficiently small to keep the stable fluctuations within the range described by their leading moments. If the diffusion is weak and there is a strong forcing of the low modes, the reduced formulas for the thresholds correctly indicate the transition but need to include higher-order corrections. Infinite-dimensional stochastic calculus gives the context for such asymptotic limits [20]. The amplitude equation results show how the higher-order terms are involved in weakening the separation [36]. Recent results on stochastic reduction offer yet another take on the remainder issue [37].

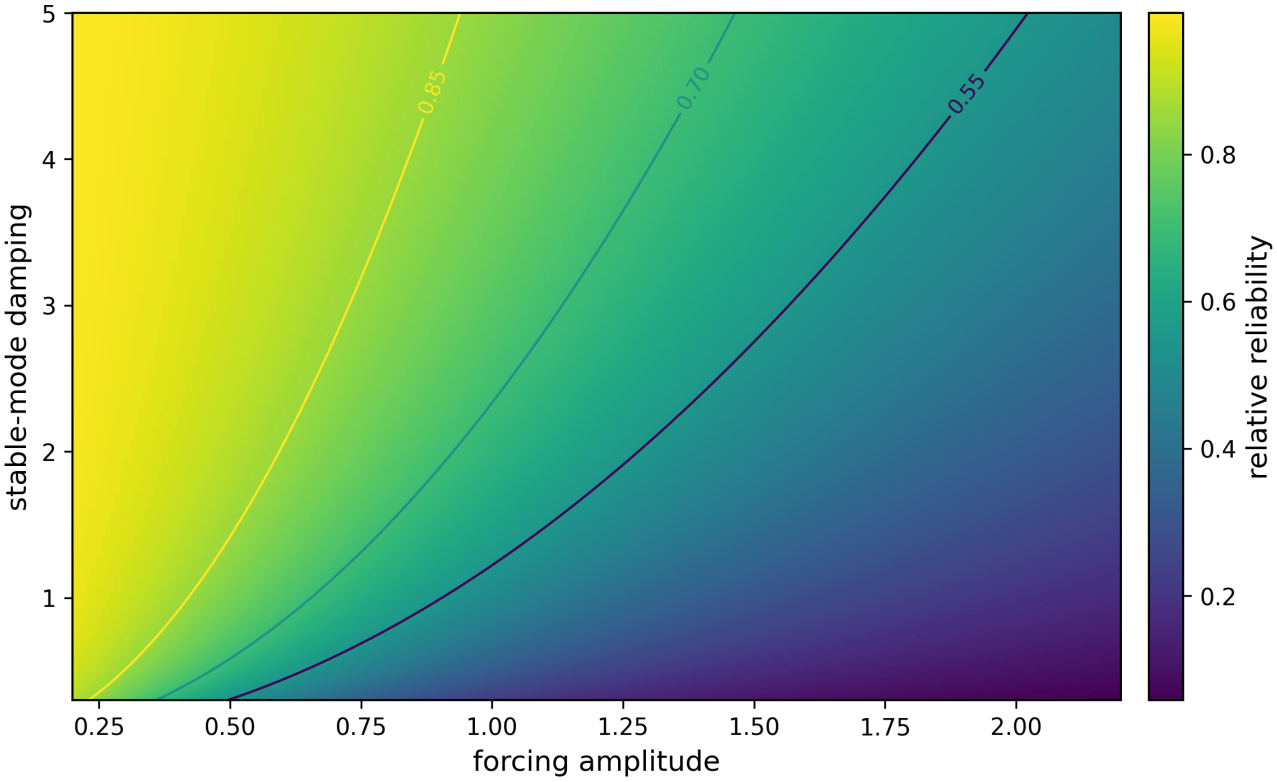

Figure 10: Reduction reliability contour.

The reliability contour of Figure 10 demarcates the region where the mean-field reduction is most defensible. The large effective damping, combined with moderate forcing, places the calculation in the fast-relaxation regime, such that the stable modes are captured by their stationary second moments. Low damping with high-mode forcing moves the calculation closer

to a region where higher-order terms could become relevant. The final figure thus establishes the modeling domain of the susceptibility index, instead of presenting it as a universal characterization of every corrosion process.

The modeling also establishes what must be measured for the purpose of validation. A traditional validation based solely on the mean chloride concentration, the mean roughness, and the variance of the total exposure would be incapable of testing the central prediction since none of these metrics captures the modal distribution of the forcing. An adequate validation will involve measuring the spatial exposure distribution, projecting it to a no-flux or shape-based basis, estimating the dominant-mode amplitudes, and comparing the resulting $\mathcal{S}_r$ to observed activity changes. In a laboratory study, such validation may take the form of patterned wetting, patterned salt deposition, or a set of engineered coating defects. In a field survey, it may consist of defect maps or chloride maps along the surface of the sample. The key condition is the comparison of the same total exposure under different spatial distributions.

The theory also draws a distinction between two types of corrosion risk that are commonly conflated. The local initiation risk is related to the largest local fluctuations, sharp defects, and high-activity gradients. On the other hand, the mean state susceptibility is determined by the modal variance that persists in stable modes after damping and contributes to the slow activity evolution. High local initiation risk means that a material has sharp high-mode defects, even if the mean-state susceptibility is low since those defects get dampened in the reduced model. Likewise, a broad low-intensity exposure band may have modest local severity yet high mean-field influence. The distinction helps prevent misinterpreting the reduced threshold as a description of all corrosion risks.

The identifiability of the parameters deserves care as well. The diffusion coefficient D and the fractional exponent r are not just curve-fitting parameters; they reflect the transport properties of the material and the exposure geometry in the form of scale redistribution. For their accurate estimation, either independent transport experiments or inverse modeling based on spatially resolved time series would be required. Similarly, the forcing amplitudes α_j are not the environmental concentrations. They are the stochastic amplitudes after nondimensionalization and projection to the selected basis. The 600-case grid is therefore better interpreted as an analytical record that maps the consequences of the parameters rather than a replacement of the calibration. It prevents claims beyond the theoretical derivation.

The main lesson is that corrosion data should not be reduced to total environmental variance when spatial information is available. Imaging, scanning electrochemical microscopy, surface profilometry, chloride mapping, and coating-defect surveys all yield information decomposable into spatial scales. Reviews of machine-learning approaches to corrosion already stress the importance of structured descriptors [26]. Studies in corrosion informatics advocate uncertainty-aware and physics-informed features [27]. Time series demonstrate how the temporal structure can help with initiating from propagating corrosion [28]. Environmental-atmospheric corrosion models increasingly consider both environmental and material variables in time [29]. From the point of view of physics, modal decomposition is another motivation for using the spectral descriptors since they directly affect the mean corrosion activity through the threshold index. A learned predictor can estimate the mode amplitudes or modal weights, whereas the fractional stochastic model explains how the latter affect the mean corrosion activity.

7. Conclusion

The research question of whether the spatial scale of the random exposure can be quantitatively expressed through the mean corrosion activity in a fractional reaction–diffusion system is answered affirmatively. The decisive quantity is the susceptibility index of modal amplitudes $\mathcal{S}_r = \sum_{j\in\mathcal{J}} \alpha_j^2/(2Dj^r)$ measuring the proportion of variance surviving fractional stable-mode damping and entering mean-field dynamics. The index is able to distinguish between different exposure modes with equal variance.

The passivity region of cubic passivation–activation kinetics becomes stable whenever $\mathcal{S}_r > 1/3$. The threshold can be rewritten as a critical value of the single-mode amplitude $\alpha_{\text{crit}} = \sqrt{2Dq^r/3}$, which explicitly demonstrates that diffusion, forced mode, and fractional exponent increase the exposure amplitude necessary for stabilization. In case of logistic saturated damage-growth kinetics with the critical rate $K = 1$, positive equilibria appear only for $\mathcal{S}_r \leq 1/4$. Increasing modal susceptibility squeezes the positive equilibria pair until collision of roots occurs. Thus, the two kinetic closures translate the same modal index into different interpretations of corrosion: passivity stabilization in one case and destruction of the positive equilibrium pair in the other.

The numerical analysis of 600 cases proves the importance of the modal placement in the crossing of the threshold. From 600 considered cases, 128 satisfy the cubic stability condition; from them, 75 cases correspond to the forced mode equal to one, while only two cases are related to the fifth mode. On the contrary, for logistic positive equilibria, the opposite mode structure takes place due to the fact that low modes are more likely to exceed the root collision threshold. Diffusion and fractional exponent influence on this property but do not destroy it. While the first mode is independent of the fractional

exponent r, higher modes are more and more strongly damped as r approaches the classical value of two.

In conclusion, structured environmental exposure cannot be characterized sufficiently by the total variance. The corrosion surface exposed to the broad chloride-containing band has a stronger mean-field effect than the surface with higher short-wave roughness if the broad band projects onto low modes. Such an observation justifies the introduction of spatially dependent environmental variables in corrosion models since such surface descriptors as imaging, inspection, and sensor data records can be translated into modal amplitudes.

The field equation, modal calculation grid, and threshold tables give the same answer from different sides. Equations identify the way of entrance of stable-mode variance into the mean field. The 600 calculated cases illustrate the number of times the thresholds are crossed in the given range of parameters. Figures reveal the reason why the threshold crossing is mainly governed by low modes rather than by total amplitude. This combination of results maintains the mathematical finding in relation to the measurable surface patterns such as broad chloride bands, coating-defect array, and image-based corrosion activity profile.

This result can be interpreted as a first-order theory of susceptibility. It does not predict the specific morphology of the corrosion pits, the chemical process inside a crevice, or the crack path after corrosion damage. The result identifies when structured exposure is sufficient to change the slow dynamics of a fractional activity field. Such a prediction is important since many screening and monitoring tasks require a compact criterion before performing high-fidelity modeling. The modal susceptibility index can be used as a ranking of the exposure patterns, guidance for spatial measurements, and indication of the laboratory cases suitable for mean-state shifts rather than only scatter.

Application of the result to any specific material requires calibration of the activity field against anodic current density, pit density map, corrosion product intensity, or aggressive species concentration. Then numerical simulation of the complete stochastic field can validate the threshold formula prior to transfer the model into the framework of two-dimensional geometry, non-Gaussian forcing, and electrochemical variables coupling. However, the central idea remains the same: the spatial spectrum of environmental fluctuations is a crucial variable in fractional dynamics of corrosion activity.

References

[1] Faulkner, L. R., & Bard, A. J. (2000). Electrochemical methods: fundamentals and applications. Wiley.
[2] Newman, J., & Thomas-Alyea, K. E. (2004). Electrochemical Systems, Wiley.
[3] Landolt, D. (2007). Corrosion and surface chemistry of metals. EPFL press.
[4] Frankel, G. S. (1998). Pitting corrosion of metals: a review of the critical factors. Journal of the Electrochemical society, 145(6), 2186-2198.
[5] Frankel, G. S., & Sridhar, N. (2008). Understanding localized corrosion. Materials today, 11(10), 38-44.
[6] McCafferty, E. (2010). Introduction to corrosion science. Springer Science & Business Media.
[7] Angst, U., Elsener, B., Larsen, C. K., & Vennesland, Ø. (2009). Critical chloride content in reinforced concrete—A review. Cement and concrete research, 39(12), 1122-1138.
[8] Broomfield, J. P. (2023). Corrosion of steel in concrete: understanding, investigation and repair. Crc Press.
[9] Bertolini, L., Elsener, B., Pedeferri, P., Redaelli, E., & Polder, R. B. (2013). Corrosion of steel in concrete: prevention, diagnosis, repair. John Wiley & Sons.
[10] Murray, J. D. (2002). Mathematical biology: I. An introduction. Interdisciplinary applied mathematics. Mathematical Biology, Springer, 17.
[11] Smoller, J. (2012). Shock waves and reaction—diffusion equations (Vol. 258). Springer Science & Business Media.
[12] Samko, S. G. (1993). Fractional integrals and derivatives. Theory and applications.
[13] Podlubny, I. (1999). Fractional differential equations. San Diego: Acad. Press.
[14] Metzler, R., & Klafter, J. (2000). The random walk's guide to anomalous diffusion: a fractional dynamics approach. Physics reports, 339(1), 1-77.
[15] Mainardi, F. (2010). Fractional calculus and waves in linear viscoelasticity, Imperial College Press, London.
[16] Di Nezza, E., Palatucci, G., & Valdinoci, E. (2012). Hitchhiker's guide to the fractional Sobolev spaces. Bulletin des sciences mathématiques, 136(5), 521-573.
[17] Lischke, A., Pang, G., Gulian, M., Song, F., Glusa, C., Zheng, X., ... & Karniadakis, G. E. (2020). What is the fractional Laplacian? A comparative review with new results. Journal of Computational Physics, 404, 109009.
[18] Arnold, L. (2006). Random dynamical systems. In Dynamical Systems: Lectures Given at the 2nd Session of the Centro Internazionale Matematico Estivo (CIME) held in Montecatini Terme, Italy, June 13–22, 1994 (pp. 1-43). Berlin, Heidelberg: Springer Berlin Heidelberg.
[19] Gardiner, C. (2009). Stochastic methods (Vol. 4). Springer Berlin Heidelberg.
[20] Da Prato, G., & Zabczyk, J. (2014). Stochastic equations in infinite dimensions. Cambridge university press.
[21] Prévôt, C., & Röckner, M. (2007). A concise course on stochastic partial differential equations. Berlin, Heidelberg: Springer Berlin Heidelberg.
[22] Bensoussan, A., Lions, J. L., & Papanicolaou, G. (2011). Asymptotic analysis for periodic structures (Vol. 374). American Mathematical Soc..
[23] Pavliotis, G., & Stuart, A. (2008). Multiscale methods: averaging and homogenization. Springer Science & Business Media.
[24] Berglund, N., & Gentz, B. (2006). Noise-induced phenomena in slow-fast dynamical systems: a sample-paths approach. London: Springer London.
[25] Khasminskii, R. (2011). Stochastic stability of differential equations (Vol. 66). Springer Science & Business Media.
[26] Nash, W., Drummond, T., & Birbilis, N. (2018). A review of deep learning in the study of materials degradation. npj Materials Degradation, 2(1), 37.
[27] Coelho, L. B., Zhang, D., Van Ingelgem, Y., Steckelmacher, D., Nowé, A., & Terryn, H. (2022). Reviewing machine learning of corrosion prediction in a data-oriented perspective. npj Materials Degradation, 6(1), 8.
[28] Jiang, X., Yan, Y., & Su, Y. (2022). Data-driven pitting evolution prediction for corrosion-resistant alloys by time-series analysis. npj Materials Degradation, 6(1), 92.
[29] Chen, Q., Wang, H., Ji, H., Ma, X., & Cai, Y. (2024). Data-driven atmospheric corrosion prediction model for alloys based on a two-stage machine learning approach. Process Safety and Environmental Protection, 188, 1093-1105.
[30] Jones, D. A. (1996). Principles and prevention of corrosion. (No Title).
[31] Revie, R. W. (Ed.). (2011). Uhlig's corrosion handbook. John Wiley & Sons.

[32] Henry, D. (2006). Geometric theory of semilinear parabolic equations. Springer.
[33] Temam, R. (2012). Infinite-dimensional dynamical systems in mechanics and physics. Springer Science & Business Media.
[34] Fisher, R. A. (1937). The wave of advance of advantageous genes. Annals of eugenics, 7(4), 355-369.
[35] AN, K. (1937). Étude de l'équation de la diffusion avec croissance de la quantité de matière et son application à un problème biologique. Bull Univ État Moscou Sér Int A, 1, 1-26.
[36] Blömker, D., Hairer, M., & Pavliotis, G. A. (2005). Modulation equations: Stochastic bifurcation in large domains. Communications in mathematical physics, 258(2), 479-512.
[37] Li, L., Chen, Z., & Caraballo Garrido, T. (2022, July). Dynamics of a stochastic fractional nonlocal reaction-diffusion model driven by additive noise. AIMS.